Electronic Supplementary Material (ESI) for Chemical Communications
This journal is © The Royal Society of Chemistry 2013

Supporting Information

Spin-triplet excitons in 1,3-diphenyl-7-(fur-2-yl)-1,4-dihydro-1,2,4-benzotriazin-4-yl

Christos P. Constantinides,[a] Emma Carter,[b] Damien M. Murphy,[b] Maria Manoli,[a] Gregory M. Leitus,[c] Michael Bendikov,[c] Jeremy M. Rawson[d] and Panayiotis A. Koutentis*,[a]

[a] *Department of Chemistry, University of Cyprus, P.O. Box 20537, 1678, Nicosia, Cyprus. Fax: +357 22892809; Tel:+357 22892783; E-mail: koutenti@ucy.ac.cy*

[b] *The School of Chemistry, Cardiff University, Main Building, Park Place, Cardiff, UK CF10 3AT*

[c] *Department of Organic Chemistry, Weizmann Institute of Science, 76100 Rehovot, Israel*

[b] *Department of Chemistry & Biochemistry, University of Windsor, 401 Sunset Avenue, Windsor, ON, Canada N9B 3P4*

Electronic Supplementary Material (ESI) for Chemical Communications
This journal is © The Royal Society of Chemistry 2013

Supporting Information

Figure S1. Cyclic voltammogram of radical **1** (1 mM), *n*-Bu_4NPF_6 (0.1 M), CH_2Cl_2, r.t., 50 mV/S.

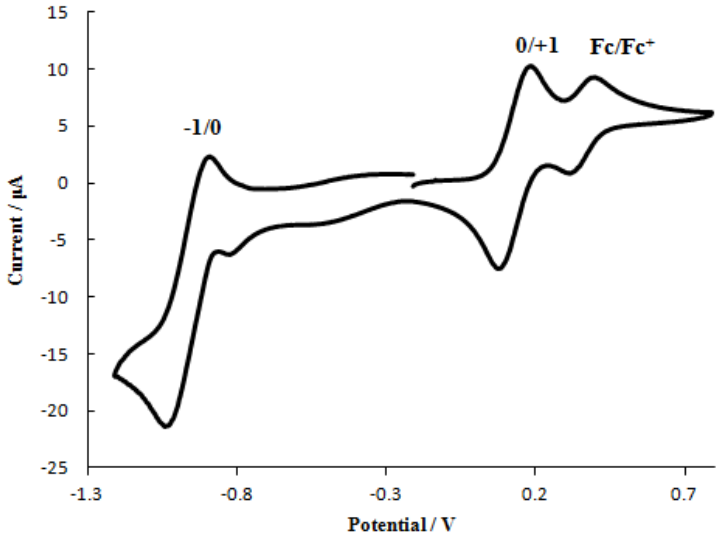

Figure S2 Experimental and simulated EPR spectrum of radical **1** at r.t. in CH_2Cl_2.

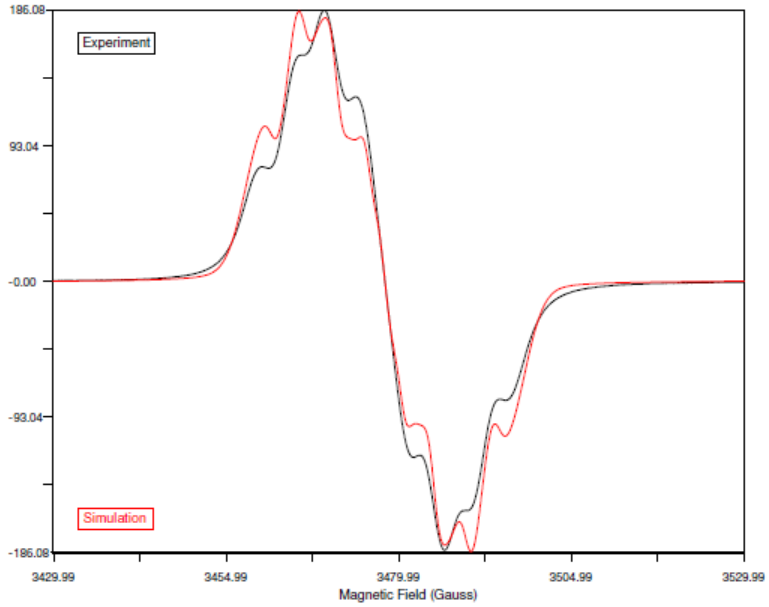

Note: Previous EPR studies on the Blatter radical and its 3-*tert*-butyl derivative, carried out by Neugebauer, showed that the spin density was mainly delocalized on the amidrazonyl fragment of the 1,2,4-triazinyl cycle.[1] The largest hyperfine coupling

constant (hfcc) was clearly assigned to the N1 atom (~7.50 G) by ^{15}N labelling.[1b,d] The N2 and N3 coupling constants are smaller and approximately equal to each other (~5.1 G). Simulations of EPR spectra of Blatter radical and its 3-*tert*-butyl derivative ^{15}N labelled in 3-position, indicated that the hyperfine coupling constant at N3 was larger than the coupling constant at N2. This assignment was unambiguously confirmed by ENDOR spectra of [3-^{15}N]-labelled Blatter radical and [4-^{15}N]-labelled 3-*tert*-butyl derivative and found hfcc *a*(N3) ~ 5.10 G and *a*(N2) ~ 4.80 G.[1c]

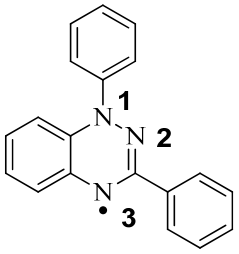

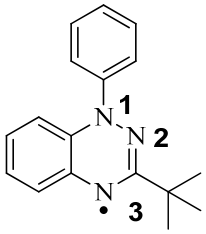

Blatter Radical

Assignment of hyperfine coupling constants for radical **1** are given according to Neugebauer's EPR work; *a*(N1) = 7.06, *a*(N2) = 4.53 and *a*(N3) = 4.75 G

Figure S3. Geometry of radical **1** in the crystal and the crystallographic atom numbering that is used in the discussion of the X-ray structure, which differs from IUPAC. Thermal ellipsoids are shown at 50% probability.

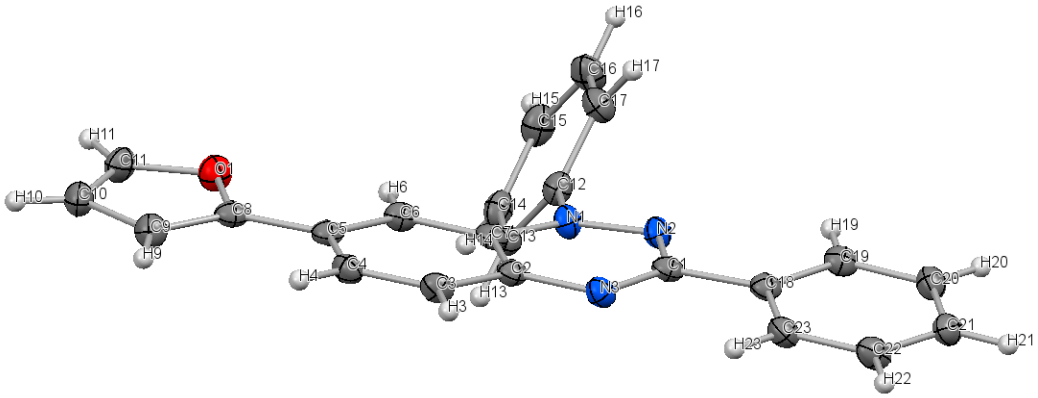

Figure S4. Packing of radical **1** along the *b* axis showing the formation of 1D chain of π-slipped radicals with alternate distances.

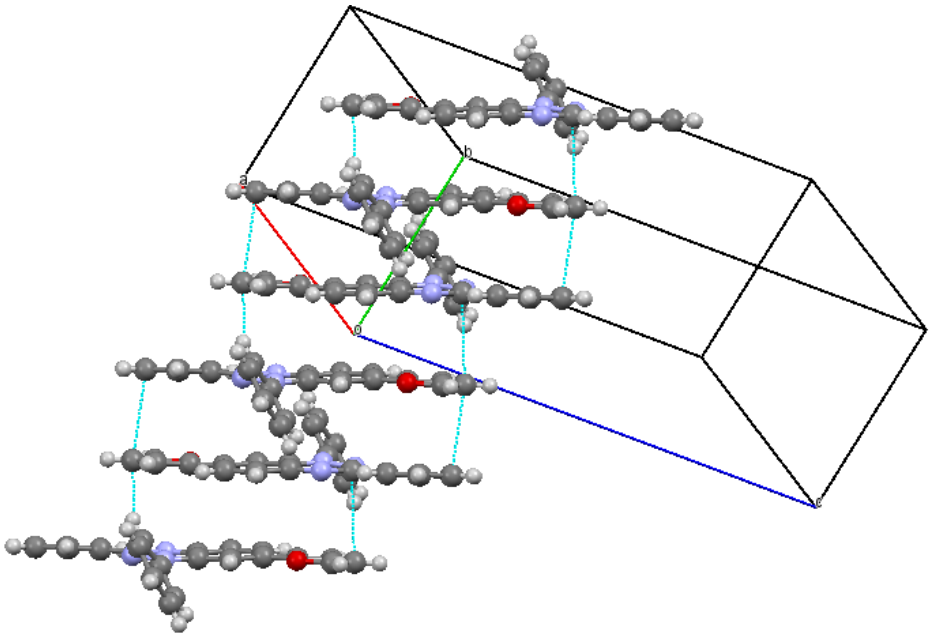

This journal is © The Royal Society of Chemistry 2013

Figure S5. CW EPR spectra of radical **1**, recorded at 5-80 K. Spectra are expanded to highlight the triplet resonance lines marked by asterisks (*)

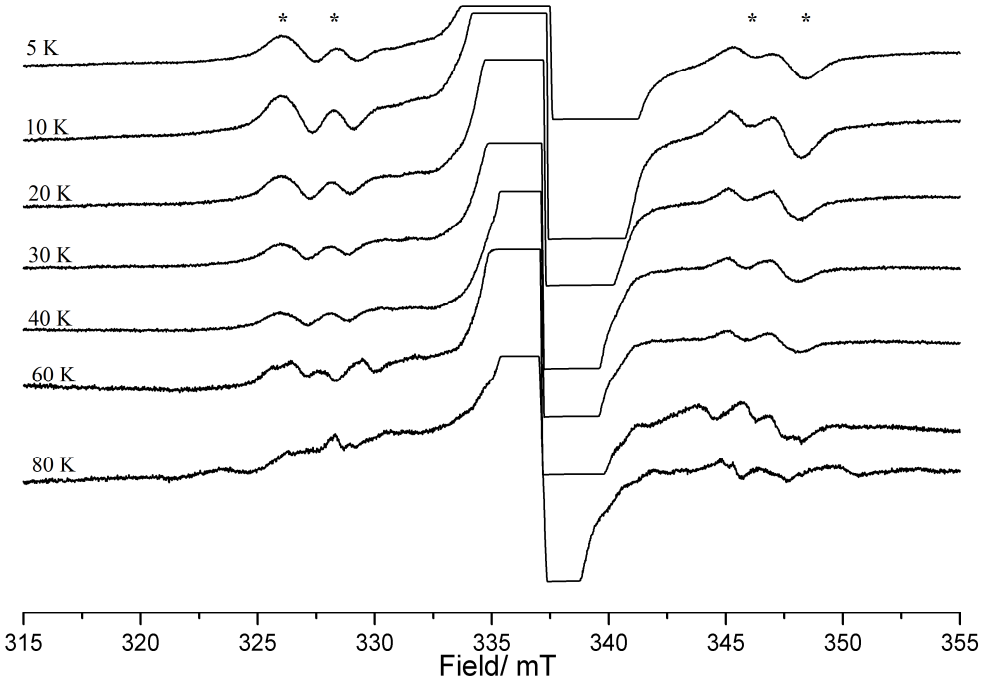

Figure S6. CW EPR spectra of radical **1** recorded at 140-260 K.

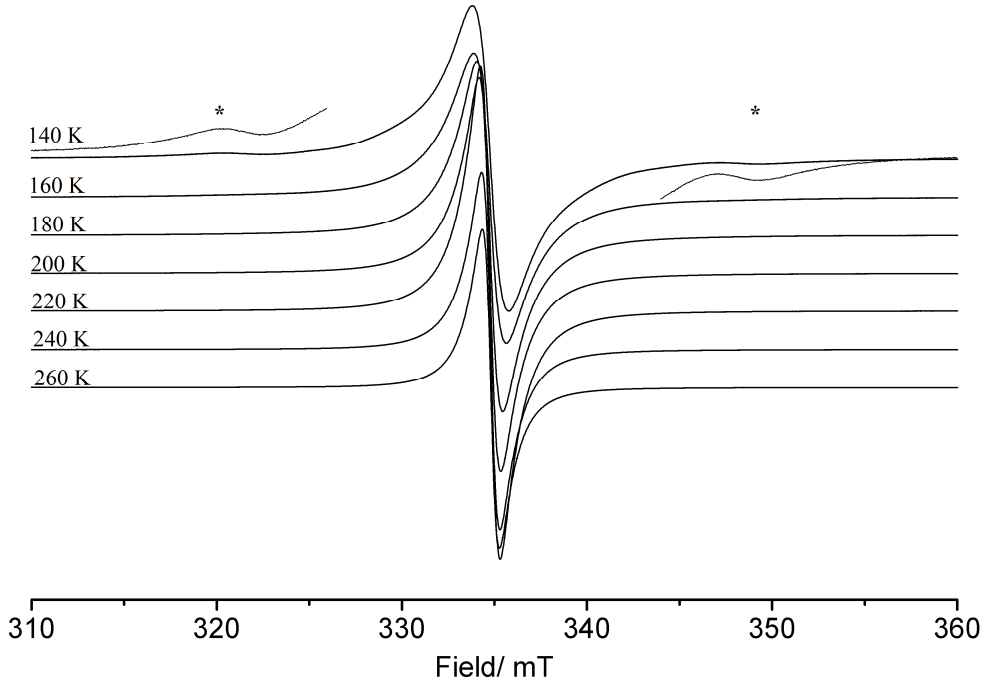

This journal is © The Royal Society of Chemistry 2013

Table T1. Mean interplanar distances and longitudinal slippage angles in pair I-II and dimer II-III of radical **1**

Temperature (K)	Pair I-II		Dimer II-III	
	d (Å)	φ (^{o})	d (Å)	φ (^{o})
100	3.396	44.4	3.413	11.4
160	3.417	44.3	3.438	11.7
300	3.475	44.4	3.489	12.8

Table T2. Energies of triplet (E_T) and broken symmetry singlet (E_{BS}) states along with spin contaminations before $\langle S^2 \rangle$ and after $\langle S^2_A \rangle$ annihilation calculated on the X-ray determined geometries (100, 160 and 300 K) at the UB3LYP/6-311G++(d,p) level of theory.

Dimer	T (K)	Triplet state			BS singlet state		
		E_T (a.u.)	$\langle S^2 \rangle$	$\langle S^2_A \rangle$	E_{BS} (a.u.)	$\langle S^2 \rangle$	$\langle S^2_A \rangle$
I-II	100	-2250.9104709	2.03	2.00	-2250.9104561	1.03	0.25
II-III	100	-2250.9068697	2.03	2.00	-2250.9079805	0.98	0.22
I-II	160	-2250.9105245	2.03	2.00	-2250.9105102	1.03	0.24
II-III	160	-2250.9074984	2.03	2.00	-2250.9084707	0.99	0.22
I-II	300	-2250.9036298	2.03	2.00	-2250.9036148	1.03	0.24
II-III	300	-2250.9012609	2.03	2.00	-2250.9019041	1.00	0.23

Table T3. Calculated exchange interactions of pair I-II ($2\boldsymbol{J}_{I\text{-}II}$) and dimer II-III ($2\boldsymbol{J}_{II\text{-}III}$) on the X-ray determined geometries at the UB3LYP/6-311G++(d,p) level of theory.

Temperature (K)	$2\boldsymbol{J}_{I\text{-}II}$ (cm^{-1})	$2\boldsymbol{J}_{II\text{-}III}$ (cm^{-1})
100	+3.2	-243.8
160	+3.1	-213.4
300	+3.3	-141.2

This journal is © The Royal Society of Chemistry 2013

Table T4. Spin Hamiltonian parameters for the S = 1/2 and S = 1 states of radical **1** calculated at 5 K.

Spin	g_x	g_y	g_z	A_x (MHz)	A_y (MHz)	A_z (MHz)	D (cm^{-1})	E (cm^{-1})
1/2	2.002	2.002	2.0080	7	10	20	-	-
1	2.0035	2.0035	2.0080	7	10	20	0.018	0.001

Instrumental Analysis

CH_2Cl_2 freshly distilled from CaH_2 under argon. DMF was azeotropically distilled with PhH then distilled under vacuum from anhydrous $MgSO_4$ and stored over 4 Å molecular sieves. Anhydrous Na_2SO_4 was used for drying organic extracts, and all volatiles were removed under reduced pressure. All reaction mixtures and column eluents were monitored by TLC using commercial aluminium backed thin layer chromatography (TLC) plates (Merck Kieselgel 60 F_{254}). The plates were observed under UV light at 254 and 365 nm. The technique of dry flash chromatography was used throughout for all non-TLC scale chromatographic separations using Merck Silica Gel 60 (less than 0.063 mm). Melting points were determined using a PolyTherm-A, Wagner & Munz, Koefler-Hotstage Microscope apparatus. Solvents used for recrystallization are indicated after the melting point. UV spectra were obtained using a Perkin-Elmer Lambda-25 UV/*vis* spectrophotometer and inflections are identified by the abbreviation "inf". IR spectra were recorded on a Shimidazu FTIR-NIR Prestige-21 spectrometer with Pike *Miracle* Ge ATR accessory and strong, medium and weak peaks are represented by s, m and w respectively. Low resolution (EI) mass spectra were recorded on a Shimadzu Q2010 GCMS with direct inlet probe. Cyclic voltammetry (CV) measurements were performed on a Princeton Applied Research Potentiostat/Galvanostat 263A apparatus. The concentration of the benzotriazinyl radical used was 1 mM in CH_2Cl_2. A 0.1 M CH_2Cl_2 solution of tetra-butylammonium hexafluorophosphate ($TBAPF_6$) was used as electrolyte. The reference electrode was Ag/AgCl and the scan rate was 50 mV/s. Ferrocene was used as an internal reference; the $E_{1/2}$(ox) of ferrocene in this system was 0.352 V.[2] Solution EPR spectra were recorded on a Bruker ESP-300E EPR spectrometer running at X-band

(~ 9.77 GHz) at room temperature. Accurate microwave frequencies were measured using a microwave counter. The spectrum recorded in both first and second derivative modes on solutions in CH_2Cl_2 and simulations undertaken with Winsim[3] using a pure Gaussian lineshape with linewidths of *ca*. 2 G. Generally better resolution and estimates of hyperfine couplings were afforded by the second derivative spectra. The solid-state VT-EPR spectra were recorded on an X-band (~ 9 GHz) *Bruker EMX* spectrometer operating at 100 kHz field modulation, 10 mW microwave power and fitted with a high sensitivity cavity (ER 4119HS). The spectrometer is equipped with a variable temperature unit to allow measurements to be performed at temperatures ranging from 120 K to 298 K. ***g*** values were determined using a DPPH standard. A small quantity of the solid (polycrystalline) radical **1** was loaded into high-quality suprasil EPR tubes. The low temperature (5 – 120 K) CW EPR spectra were recorded on an X-band Bruker ESP300e series spectrometer using 12.5 kHz field modulation, 2.5 mW microwave power and fitted with a Bruker ENDOR cavity (801en358). EPR simulations were performed using the Easyspin toolbox for Matlab.[4] X-ray data of radical **1** (CCDC 947823) were collected on an Oxford-Diffraction Supernova diffractometer, equipped with a CCD area detector utilizing Mo-Kα radiation (λ = 0.71073 Å). A suitable crystal was attached to glass fibers using paratone-N oil and transferred to a goniostat where they were cooled for data collection. Unit cell dimensions were determined and refined by using 2949 ($3.24 \leq \theta \leq 25.00^{o}$) reflections. Empirical absorption corrections (multi-scan based on symmetry-related measurements) were applied using CrysAlis RED software.[5] The structures were solved by direct method and refined on F^2 using full-matrix least squares using SHELXL97.[6] Software packages used: CrysAlis CCD[4] for data collection, CrysAlis RED[4] for cell refinement and data reduction, WINGX for geometric calculations,[7] and Mercury 3.1[8] for molecular graphics. The non-H atoms were treated anisotropically. The hydrogen atoms were placed in calculated, ideal positions and refined as riding on their respective carbon atoms. DFT calculations were performed using the Gaussian 03 suite of programs.[9]

Experimental procedures and spectral analysis:

*1,3-Diphenyl-7-(fur-2-yl)-1,4-dihydro-1,2,4-benzotriazin-4-yl (**1**)*[10]

A stirred mixture of 7-iodo-1,3-diphenyl-1,4-dihydro-1,2,4-benzotriazinyl (**2**) (50 mg, 0.122 mmol), fur-2-ylSnBu$_3$ (2 equiv.) and Pd(OAc)$_2$ (5 mol%) was heated to *ca.* 100 ^{o}C in dry DMF (2 mL) for 0.5 h under inert conditions until all the starting material was consumed (TLC). Dry flash chromatography (Et$_2$O/*n*-hexane, 1:3) of the reaction mixture gave the title compound **1** in 82% yield as red needles, mp 163-165 ^{o}C (lit.,[9] 163-165 ^{o}C). (Found: C, 78.86; H, 4.67; N, 11.97. $C_{23}H_{16}N_3O$ requires C, 78.84; H, 4.60; N, 11.99%); g = 2.0071; λ_{max}(DCM) 309 (log ε 3.73), 401 (2.98), 433 (2.91), 459 (2.80), 507 (2.50), 541 (2.75); ν_{max}/cm^{-1} 3062vw, 1593w, 1508w, 1487w, 1454w, 1392m, 1317w, 1222w, 1172w, 1047w, 1016w, 817w, 783m; *m/z* (EI) 351 (M^+ + 1, 32%), 350 (M^+, 100), 142 (19), 92 (13), 77 ($C_6H_5^+$, 20), 51 (10).

Crystal refinement data radical **1** (CCDC 947823) (100 K, red-brown needles): $C_{23}H_{16}N_3O$, M = 350.39, monoclinic, space group $P\ 2_1/n$, a = 9.9695(7) Å, b = 8.1556(5) Å, c = 20.8837(15) Å, α = 90^{o}, β = 99.284(7)^{o}, γ = 90^{o}, V = 1675.8(2) Å^3, Z = 4, T = 100(2) K, ρ_{calcd} = 1.389 g cm^{-3}, θ_{max} = 25. Refinement of 244 parameters on 2949 independent reflections out of 8466 measured reflections (R_{int} = 0.0308) led to R_1 = 0.0447 [I>2σ(I)], wR_2 = 0.1254 (all data), and S = 1.097 with the largest difference peak and hole of 0.178 and -0.284 e^{-3}, respectively.

References

1) (*a*) K. Mukai, K. Inoue, N. Achiwa, J. B. Jamali, C. Krieger and F. A. Neugebauer, *Chem. Phys. Lett.*, 1994, **224**, 569; (*b*) F. A. Neugebauer and I. Umminger, *Chem. Ber.*, 1980, **113**, 1205; (*c*) F. A. Neugebauer and G. Rimmler, *Magn. Reson. Chem.*, 1988, **26**, 595; (*d*) F. A. Neugebauer and I. Umminger, *Chem. Ber.*, 1981, **114**, 2423.

2) M. Dietrich and J. Heinze, *J. Am. Chem. Soc.*, **1990**, 112, 5142.

3) Winsim 2002 (v.0.98), Public EPR Software Tools, D. A. O'Brien, D. R. Duling and Y. C. Fann, NIEHS, National Institutes of Health, USA.

4) S. Stoll and A. Schweiger, *J. Magn. Reson.*, 2006, **178**, 42.

5) Oxford Diffraction (2008). CrysAlis CCD and CrysAlis RED, version 1.171.32.15, Oxford Diffraction Ltd, Abingdon, Oxford, England.

6) G. M. Sheldrick, "SHELXL97-A program for the refinement of crystal structure", University of Göttingen, Germany.

7) L. J. Farrugia, "WinGX suite for single crystal small molecule crystallography", *J. Appl. Crystallogr.*, 1999, **32**, 837.

8) C. F. Macrae, P. R. Edgington, P. McCabe, E. Pidcock, G. P. Shields, R. Taylor, M. Towler and J. van de Streek, *J. Appl. Cryst.*, 2006, **39**, 453.

9) Gaussian 03, Revision C.02, M. J. Frisch, G. W. Trucks, H. B. Schlegel, G. E. Scuseria, M. A. Robb, J. R. Cheeseman, J. A. Montgomery, Jr., T. Vreven, K. N. Kudin, J. C. Burant, J. M. Millam, S. S. Iyengar, J. Tomasi, V. Barone, B. Mennucci, M. Cossi, G. Scalmani, N. Rega, G. A. Petersson, H. Nakatsuji, M. Hada, M. Ehara, K. Toyota, R. Fukuda, J. Hasegawa, M. Ishida, T. Nakajima, Y. Honda, O. Kitao, H. Nakai, M. Klene, X. Li, J. E. Knox, H. P. Hratchian, J. B. Cross, V. Bakken, C. Adamo, J. Jaramillo, R. Gomperts, R. E. Stratmann, O. Yazyev, A. J. Austin, R. Cammi, C. Pomelli, J. W. Ochterski, P. Y. Ayala, K. Morokuma, G. A. Voth, P. Salvador, J. J. Dannenberg, V. G. Zakrzewski, S. Dapprich, A. D. Daniels, M. C. Strain, O. Farkas, D. K. Malick, A. D. Rabuck, K. Raghavachari, J. B. Foresman, J. V. Ortiz, Q. Cui, A. G. Baboul, S. Clifford, J. Cioslowski, B. B. Stefanov, G. Liu, A. Liashenko, P. Piskorz, I. Komaromi, R. L. Martin, D. J. Fox, T. Keith, M. A. Al-Laham, C. Y. Peng, A. Nanayakkara, M. Challacombe, P. M. W. Gill, B. Johnson, W. Chen, M. W. Wong, C. Gonzalez, and J. A. Pople, Gaussian, Inc., Wallingford CT, 2004.

10) C. P. Constantinides, P. A. Koutentis and G. Loizou, *Org. Biomol. Chem.*, 2011, **9**, 3122.